Laser-Induced Fluorescence Spectra and Torsional Potential Energy Functions of Jet-Cooled 4,4′-Dimethyl-*trans*-Stilbene†

Zane Arp,‡ Whe-Yi Chiang,‡ Jaan Laane,*,‡ Akira Sakamoto,§ and Mitsuo Tasumi§

Department of Chemistry, Texas A&M University, College Station, Texas 77843-3255, and Department of Chemistry, Faculty of Science, Saitama University, Saitama 338-8570, Japan

Received: July 11, 2001; In Final Form: September 25, 2001

The laser-induced fluorescence excitation spectra of jet-cooled 4,4′-dimethyl-*trans*-stilbene have been recorded, and the phenyl and methyl internal rotation levels have been assigned for the S_0 and the $S_1(\pi,\pi^*)$ electronic states. Dispersed fluorescence spectra and vapor-phase Raman spectra were utilized to help assign the low-frequency vibrations in the electronic ground state. The methyl torsions have energy levels and potential functions very similar to those of *m*-xylene. The S_0 state has $V_6 = 15 \pm 15$ cm^{-1} (negligible barrier), while S_1 has $V_3 = 85 \pm 10$ cm^{-1} and $V_6 = -30 \pm 20$ cm^{-1}. The barrier to simultaneous internal rotation of the phenyl groups in S_0 was found to be 3100 cm^{-1}. This is identical to that of *trans*-stilbene within experimental error. For the S_1 state, the barrier is 3140 cm^{-1} as compared to 3000 cm^{-1} for *trans*-stilbene. The barrier to rotation about the C═C bond in the S_0 state was estimated to be 41 ± 5 kcal/mol based on one assigned frequency. In the S_1 state the *trans*-twist barrier was estimated to be approximately 2400 cm^{-1}.

Introduction

Stilbene and its derivatives have been of considerable interest to both experimental and theoretical chemists for more than 2 decades.[1,2] These molecules tend to show strong fluorescence and they can undergo photoisomerization in their electronic excited states. Chiang and Laane have previously reported the fluorescence spectra of jet-cooled *trans*-stilbene[2] and 4-methoxy-*trans*-stilbene[3] and determined potential energy functions for both the phenyl torsions and the torsion about the C═C bond which governs the photoisomerization.

In the present paper we present the fluorescence excitation spectra and dispersed fluorescence spectra of jet-cooled 4,4′-dimethyl-*trans*-stilbene (DMS). Vapor-phase Raman spectra of the sample at high temperature were also recorded to complement the studies. This molecule possesses internal rotations about the C−CH_3 bonds in addition to the three torsional motions in the unsubstituted *trans*-stilbene adding considerable complexity to the spectra. The analysis of the data presented here will provide insight into the effect (or lack of effect) that substitution on the benzene rings has on the torsional processes.

Experimental Section

The compound 4,4′-dimethyl-*trans*-stilbene (DMS) was prepared in Japan according to the method of Drefahl and Ploetner.[4] The integrity of the sample was verified by infrared spectroscopy. The laser-ininduced fluorescence spectra were recorded in Texas using the system previously described.[2,5,6] This system now utilizes a Continuum Powerlite 9020 Nd:YAG laser and a Continuum Sunlite OPO laser with an FX-1 UV extension unit as the tunable excitation source. Dispersed spectra were recorded using an ISA HR-640 monochromator and a Spex Spectrum One CCD detector (2000 × 800 pixels). Vapor-phase Raman spectra were recorded using the methodology and cells previously described.[7]

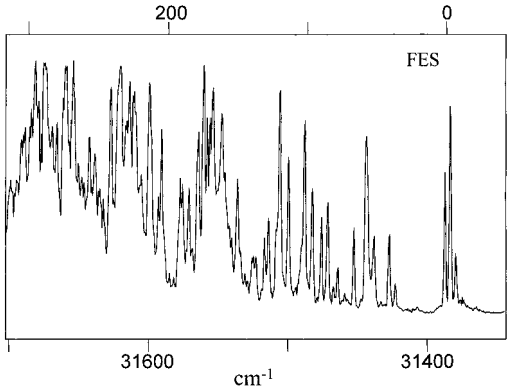

Figure 1. Fluorescence excitation spectrum of DMS.

Fluorescence Spectra. Figure 1 shows the laser induced fluorescence excitation spectrum of DMS in the low-frequency region. Table 1 lists the observed wavenumbers (cm^{-1}) along with assignments. The numbering of the vibrations used for *trans*-stilbene[2] in C_{2h} symmetry is maintained. Nomenclature for labeling the transitions due to the methyl torsions is described below. The other four low-frequency methyl vibrations (the in-plane and out-of-plane wags expected in the 300−400 cm^{-1} region for both the S_0 and S_1 states) are also not included in the numbering system for the vibrations. Thus, while *trans*-stilbene has eight low-frequency vibrational modes, as described previously,[2] DMS has six additional ones due to the introduction of the methyl groups.

Thus, the fluorescence excitation spectrum of DMS is very rich due to the many low-frequency modes. DMS has 60 clearly observed excitation bands below 240 cm^{-1} whereas *trans*-stilbene has only 30.

Near the electronic origin at 37 386 cm^{-1} three bands can be seen. These are due to the transitions between the lowest methyl torsional levels in the two electronic states. As will be shown,

† Part of the special issue "Mitsuo Tasumi Festschrift".
‡ Department of Chemistry, Texas A&M University.
§ Department of Chemistry, Faculty of Science.

10.1021/jp012607n CCC: $22.00
Published on Web 11/22/2001

TABLE 1: Fluorescence Excitation Spectrum (cm^{-1}) of Dimethyl-*trans*-stilbene

observed[a]	Inferred	assignment
−31 (5)	−30	$37_4^0\,M_{11}^{11}$
−26 (8)	−26	$37_4^0\,M_{01}^{01}$
−22 (3)	−22	37_4^0
−17 (3)	−17	$37_2^0\,M_{11}^{11}$
−14 (5)	−13	$37_2^0\,M_{01}^{01}$
−7.5 (38)	−7.5	M_{11}^{11}
−3.7 (100)	−3.7	M_{01}^{01}
0.0 (69)	0	$0_0^0(M_{00}^{00})$
18 (6)	18	M_{02}^{02}
26 (6)	24	37_2^2
30.2 (8)	30.1	M_{11}^{12}
33.8 (6)	33.8	M_{01}^{02}
36 (17)	36	$36_0^1\,37_3^0$
40.3 (36)	41	$37_4^4\,M_{01}^{01}$
47 (9)	46.6/46	$M_{10}^{13}/37_0^4\,M_{02}^{01}$
51.3 (31)	50.4/51.5	M_{00}^{03}/M_{12}^{22}
56.9 (72)	57/56/58/58	$36_0^1\,37_4^3/37_2^2\,M_{11}^{12}/37_0^4\,M_{11}^{11}/37_2^2\,M_{01}^{02}$
61 (11)	62	$37_0^4\,M_{01}^{01}$
65.8 (44)	(65.7)	37_0^4
72 (9)	73	M_{01}^{14}
77.4 (36)	78/77.2	$36_0^1\,37_0^3/M_{00}^{04}$
80 (11)	80.4/80.5	$48_0^2\,37_0^4/M_{02}^{05}$
82 (11)	82	$36_0^2\,M_{11}^{11}$
84.8 (57)	85.7	$36_0^2\,M_{01}^{01}$
89.3 (47)	(89.4)/90	$36_0^2/37_2^6$
95.9 (56)	96.6/94.9	M_{01}^{05}/M_{02}^{24}
101.4 (72)	(101.4)	48_0^2
103 (22)	102	$36_0^2\,37_4^2$
112.6 (59)	111/111/114/111	$36_0^1\,37_0^5/37_4^8/36_0^2\,37_2^2/M_{01}^{24}$
116 (26)	116/115	$36_0^2\,37_0^2\,M_{11}^{11}/25_0^1\,M_{11}^{11}$
119.2 (89)	118/119	$36_0^2\,37_0^2\,M_{01}^{01}/25_0^1\,M_{01}^{01}$
122.3 (25)	123/(122)/123	$37_2^8/25_0^1/36_0^2\,37_0^2$
127.2 (38)	126/127	$36_0^3\,37_0^3/M_{02}^{06}$
130.1 (35)	132/130	$37_0^6/M_{11}^{25}$
136 (23)	135	$36_0^2\,37_4^4$
139 (22)	139.3	M_{11}^{16}
144 (16)	144/143	$36_0^1\,37_0^7/M_{01}^{06}$
147 (19)	146/146	$37_4^4\,48_0^2/35_0^1\,36_0^1\,37_4^2$
149.2 (52)	150	$36_0^4\,37_0^4\,M_{11}^{11}$
155.8 (42)	156/157	$36_0^2\,37_0^4/35_0^2\,37_4^0$
161 (80)	161/162/160	$M_{12}^{26}/37_0^8\,M_{11}^{12}/36_0^3\,37_3^0\,M_{01}^{02}$
163 (63)	164/164	$48_0^2\,37_0^4\,M_{01}^{01}$
168 (94)	168	$36_0^3\,37_0^3$
170 (64)	169	$36_0^2\,48_0^2\,37_4^0$
171 (67)	171	$35_0^2\,M_{11}^{11}$
174 (110)	174/174	$35_0^2\,M_{01}^{01}/M_{01}^{45}$
178 (68)	(178)/177	$35_0^2/M_{11}^{26}$
182 (26)	182/183	$36_0^2\,37_0^6\,M_{11}^{11}/35_0^2\,37_4^2\,M_{11}^{11}$
184 (52)	183	$37_0^4\,48_0^4$
189 (41)	189/190	$36_0^2\,37_0^6/35_0^2\,37_4^2$
191 (59)	192/191/192	$36_0^3\,35_2^5/36_0^2\,48_0^2/36_0^4\,37_4^2$
202 (14)	203	$24_0^1\,37_4^0\,M_{01}^{01}$
204 (55)	204/204	$48_0^4/36_0^5\,37_5^0$
207 (38)	207	$24_0^1\,37_4^0$
213 (88)	212/214/212	$36_0^1\,37_0^5\,48_0^1/35_0^2\,36_0^1 37_3^0/25_0^1\,36_0^2$
218 (44)	216	$36_0^5\,37_3^0$
220 (30)	220	$37_2^8\,48_0^2\,M_{01}^{01}$
222 (50)	221	$24_0^1\,M_{11}^{11}$
224 (87)	224/224	$24_0^1\,M_{01}^{01}/37_2^8\,48_0^2$
228 (88)	(228)	24_0^1

[a] Relative intensity in parentheses.

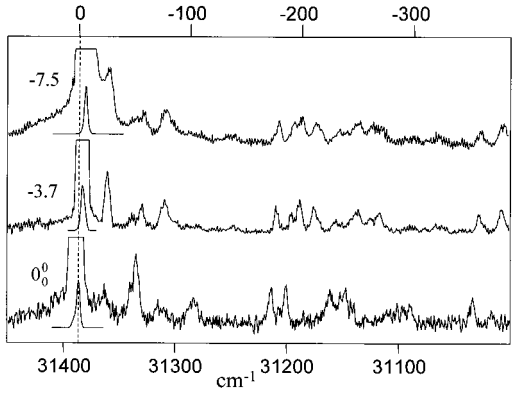

Figure 2. Single vibronic level fluorescence spectra from several excitation lines of DMS.

TABLE 2: SVLF Spectra (cm^{-1}) of Dimethyl-*trans*-stilbene

excitation lines[a]						
0	−3.7	−7.5	57	96	101	assignment[b]
0	0	0	0	0	0	0_0^0
22 w	22 s	21 s	21 s	21 s	22 vw	37_4^0
			40 s			$37_6^2\,M_{03}^{10}$
47 m	46 mw	46 w			46 vw	37_8^0
51 s	53 m	53 mw	51 m	51 m	51 w	M_{04}^{00}/M_{14}^{10}
72 w	73 m	73 m	73 m	72 s		37_{12}^0
103 ms			101 mw		101 m	48_2^0
				125 mw		$25_1^0/37_4^0\,48_2^0$
	134 w	134 w				72_2^0
173 ms	173 m	174 m	173 m	173 w	173 m	35_2^0
186 ms	187 mw	187 m	184		185 m	$35_2^0\,37_2^0$
	194 m	194 m	193 m	191		$35_2^0\,37_4^0$
	206 m	207 m	205 m		208 w	48_4^0
			212 s			47_1^0
225 ms	226 w	228 w	226 m			$35_2^0\,37_8^0$
234 ms		234 m	232 mw			$48_2^0\,72_2^0$
246 m	246 m	246 mw				$35_2^0\,37_{12}^0$

[a] Relative to 0_0^0 at 37 386 cm^{-1}. Each listed SVLF frequency is relative to its excitation frequency. [b] Assignment do not include methyl torsion components. For example, the −3.7 cm^{-1} bands typically also involve M_{01}^{01}.

in the S_0 state the methyl torsional levels are present at 5, 11, 22, 27 cm^{-1}, etc., phenyl torsional levels are at 10, 21, 33 cm^{-1}, etc., and their combinations are at 15, 21, 26, 32 cm^{-1}, etc. Hence, combinations of these levels with other vibrations gives rise to many hundreds of quantum states even at relatively low wavenumber values and many overlapping peaks show up in the spectra. Little attempt to assign the spectra much above 200 cm^{-1} was made as numerous different assignments are possible for many of the observed frequencies (see Table 1). As can be seen in Figure 1, there is broad general background fluorescence in the spectrum, presumably from the overlap of bands. This was present whether argon or helium was used as the carrier gas and at all backing pressures (1−10 atm).

Dispersed fluorescence spectra (single vibronic level fluorescence, SVLF) recorded from several different excitation lines are shown in Figure 2. While the excitation spectrum of DMS has similar intensity to *trans*-stilbene, the SVLF spectra are considerably weaker, presumably because the fluorescence is distributed between so many different vibrational levels in the ground state. Table 2 summarizes the observations from the SVLF spectra and presents assignments.

Methyl Torsions. The internal rotation of a methyl group substituted on a benzene ring is expected to have only a low

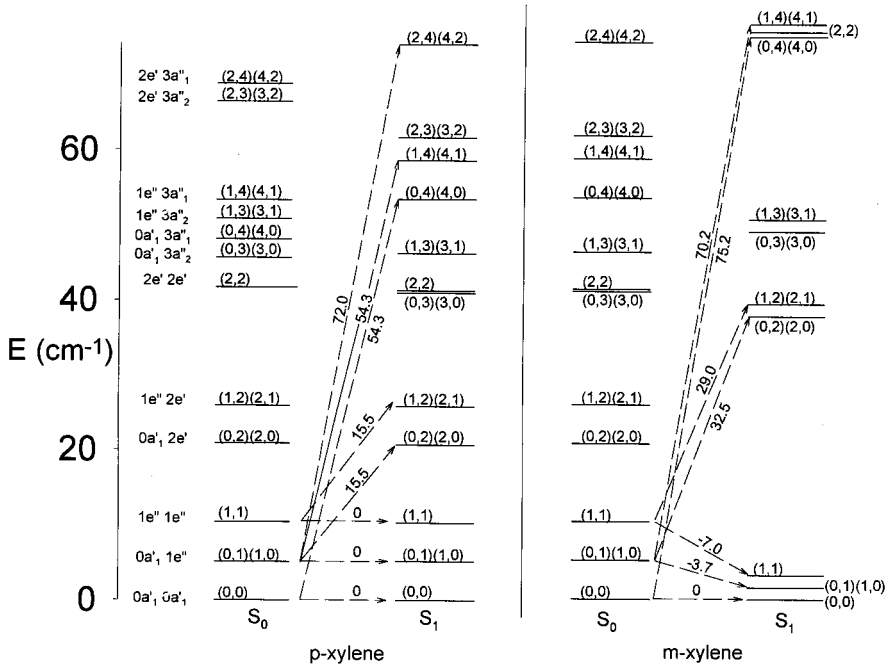

Figure 3. Methyl torsion energy levels for the S_0 and S_1 states of *p*-xylene and *m*-xylene (based on ref 8).

barrier. For two methyl groups spatially far apart the rotations can be assumed to be independent of one another, and this is the case for DMS. The torsional motion in toluene, where a C_{3v} methyl group is attached to a symmetrically substituted C_{2v} benzene ring, is governed by a 6-fold potential energy term (V_6). This is also true for each of the independent methyl rotations of *p*-xylene. For *o*-xylene or *m*-xylene, however, the asymmetric substitution on the benzene ring produces also a 3-fold potential energy term. These expectations were demonstrated for toluene and the three xylenes by Breen and co-workers[8] who recorded their laser induced fluorescence spectra. The DMS in our present study is *para*-substituted, but the attachment of the −C≡C−Ph−Me group destroys the local C_{2v} symmetry of the benzene ring and thereby can be expected to give rise to 6-fold potential terms. Hence, it is instructive to examine the methyl torsional energy levels for both *p*-xylene and *m*-xylene in their S_0 and S_1 states as reported.[8−10] Figure 3 shows the lowest quantum states for the methyl torsions for these two molecules. Both the previously used nomenclature, which shows the symmetry and helps to understand the selection rules (but is rather cumbersome), and our streamlined nomenclature are shown. Our nomenclature simply numbers the quantum states 0, 1, 2, ... for each rotor so the excitation of one quantum of the first rotor and the excitation of two for the second rotor would be labeled (1,2). An excitation from this state to a (1,1) level in S_1 is labeled as M_{12}^{11}. Figure 3 shows that *p*-xylene, which has only small 6-fold barriers for both S_0 and S_1, has torsional levels in the two electronic states which are nearly identical. Each state has the lowest torsional levels at 0 cm^{-1} (0,0), 5 cm^{-1} (0,1)(1,0), and 10 cm^{-1} (1,1). The only bands observed below 100 cm^{-1} occur at 15.5, 54.3, 72.0, and 78.1 cm^{-1} as shown in the diagram and are based on the selection rules previously discussed.[8] For *m*-xylene, the presence of the V_3 3-fold potential energy term for the S_1 state results in the (0,1)(1,0) and (1,1) levels dropping to 1.7 and 3.4 cm^{-1}, respectively. The excitation spectra then shows three transitions near the band origin: 0 cm^{-1} for (0,0) → (0,0), −3.7 cm^{-1} for (0,1)(1,0) → (0,1)(1,0), and −7.5 cm^{-1} for (1,1) → (1,1).

Examination of the DMS excitation spectrum shows that the region near the electronic origin is virtually identical to that of

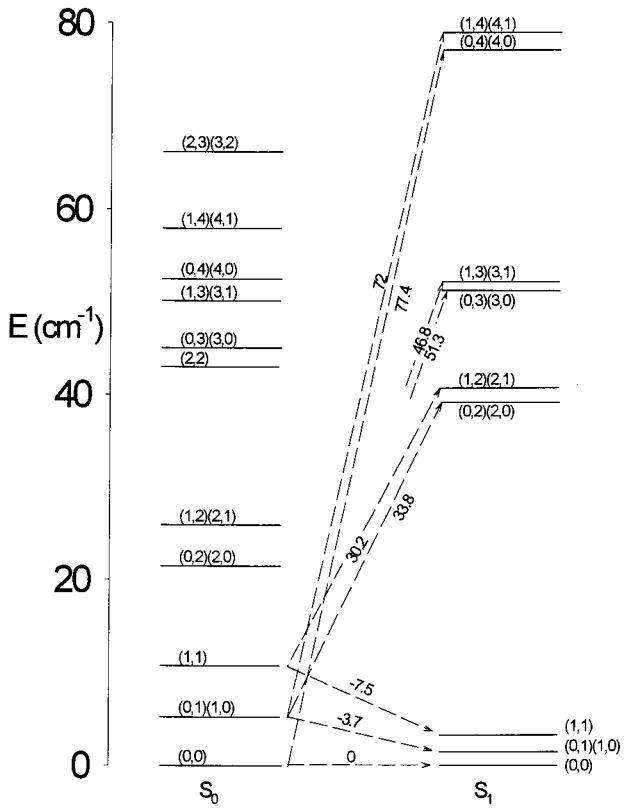

Figure 4. DMS methyl torsional quantum states and transitions for S_0 and S_1 electronic states. The transitions to the (0,3) and (1,3) are not completely shown.

m-xylene.[8−10] Even though the molecule is para-substituted, the asymmetric substitution produces a 3-fold torsional term. As in *m*-xylene the 0_0^0 band is weaker than the −3.7 cm^{-1} band since the latter is from the degenerate (0,1)(1,0) state at 5.4 cm^{-1}. The −7.5 cm^{-1} band originates from the (1,1) state at 10.7 cm^{-1} and gives rise to the weakest band of the triplet. Figure 4 shows the DMS quantum states determined from the spectra for the methyl torsions in the S_0 and S_1 states along with several of the observed transitions. Figure 5 presents the

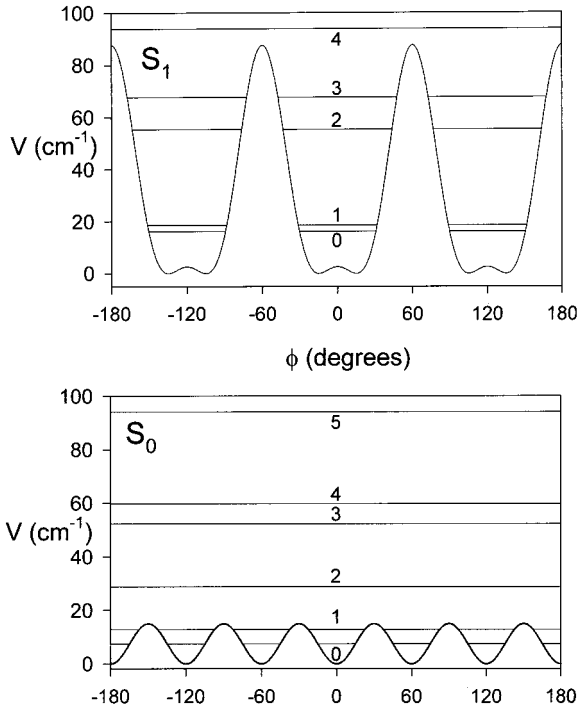

Figure 5. One-dimensional potential energy functions for a single methyl torsion in DMS in its S_0 and S_1 electronic states.

potential energy functions and quantum states for just one of the two methyl rotors in both S_0 and S_1. The levels in Figure 4 are combinations of those in Figure 5. The potential function shown in Figure 5 has the form

$$V = \frac{V_3}{2}(1 - \cos 3\phi) + \frac{V_6}{2}(1 - \cos 6\phi) \qquad (1)$$

and the energy level calculations are based on the Lewis, Chao, Malloy, and Laane[11] computational methodology. For S_0, $V_3 = 0$ and $V_6 = 15$ cm^{-1} while for S_1 $V_3 = 85$ cm^{-1} and $V_6 = -30$ cm^{-1}. The internal rotor constant is $F = 5.4$ cm^{-1} for S_0 and 5.3 cm^{-1} for S_1 (the term B is used in refs 8 and 9 instead of F, but B is generally reserved for the pseudorotor constant). Table 3 compares the observed and calculated methyl torsional frequencies and the agreement can be seen to be good. The table also presents the observed and calculated energy states. Since only the lowest energy splitting for the S_0 state and five other levels have been ascertained, the V_3 and V_6 values are not very accurately determined. V_3 is taken to be zero for the S_0 states, but values up to 5 cm^{-1} would be compatible with the observed 5.35 cm^{-1} (0,1)(1,0) state and the other values. The energy of the (0,1)(1,0) state is not very sensitive to the magnitude of V_6. The $V_6 = 15$ cm^{-1} value reproduces the observed energy levels most accurately but any value between zero and 25 cm^{-1} would reproduce them within experimental error. For the S_1 state the 3-fold barrier (as shown in Figure 5) is 85 ± 10 cm^{-1}; the uncertainty in $V_6 = -30$ is ±20 cm^{-1}. It is interesting that the methyl torsion potential functions for DMS are very similar to those of *m*-xylene but not to *p*-xylene. Evidently the symmetry of the rest of the molecule as seen by each methyl group is much more important than the position of substitution on the benzene ring.

Raman Spectra and Assignments. Figure 6 shows the vapor-phase Raman spectrum of DMS and compares it to the liquid spectrum in the same region. The spectrum of the solid is very similar to that of the liquid.[12] The vapor spectrum is particularly helpful in assigning the A_g low-frequency modes,

TABLE 3: Observed and Calculated Transition Frequencies and Energy Levels for the Methyl Torsions of Dimethyl-*trans*-stilbene

transitions (cm^{-1})			levels (cm^{-1})				
			torsional	S_0		S_1	
transition	obsd	calcd	state	obsd	calcd[a]	obsd	calcd[b]
(0,0) → (0,0)	0.0	0.0	(0,0)	0.0	0.0	0.0	0.0
(0,1) → (0,1)	−3.7	−3.7	(0,1)(1,0)	5.35	5.37	1.65	1.65
(1,1) → (1,1)	−7.5	−7.5	(1,1)	10.7	10.7	3.2	3.2
(0,2) → (0,2)	18	17.7	(0,2)(2,0)	21	21.5	39.2	39.2
(0,1) → (0,2)	33.8	33.8	(1,2)(2,1)	26.9	26.9	40.9	40.8
(1,1) → (1,2)	30.2	30.1	(0,3)(3,0)		44.9	51.3	50.4
(1,2) → (2,2)	51.3	51.5	(1,3)(3,1)		50.3	52.2	52.0
(0,0) → (0,3)	51.3	50.4	(0,4)(4,0)	52	52.5	77.2	77.2
(1,0) → (1,3)	46.8	45.1	(1,4)(4,1)		57.9	79	78.8
(0,0) → (0,4)	77.4	77.2	(2,2)		43.0	78.2	78.4
(1,0) → (1,4)	72	73.4	(2,3)(3,2)		66.4		89.6
(0,2) → (0,5)	80	80.5	(3,3)		89.8	-	100.8
(0,1) → (0,5)	95.9	96.6	(0,5)(5,0)		86.8	101.3	102.0
(0,1) → (2,4)	112.6	111	(2,4)(4,2)		74.0	117.4	116.4
(0,2) → (2,4)	95.9	94.9	(2,5)(5,2)		108.3	141.2	141.2
(0,2) → (0,6)	127.2	126.9	(0,6)(6,0)		135.2	149.1	148.4
(1,1) → (2,5)	130.1	130.5	(1,6)(6,1)		139.6	149.9	150.0
(1,1) → (1,6)	139.2	139.3	(4,5)(5,4)		139.3	179.4	179.2
(0,1) → (0,6)	143.8	143.0	(2,6)(6,2)		156.7	188.5	187.6
(1,2) → (2,6)	161	160.7					
(1,1) → (2,6)	177.8	176.9					
(0,1) → (4,5)	174.0	173.8					
(0,4) ← (0,0)	- 52	−52.5					

[a] $F = 5.4$ cm^{-1}; $V_6 = 15$ cm^{-1}. [b] $F = 5.3$ cm^{-1}; $V_3 = 85$ cm^{-1}; $V_6 = -30$ cm^{-1}.

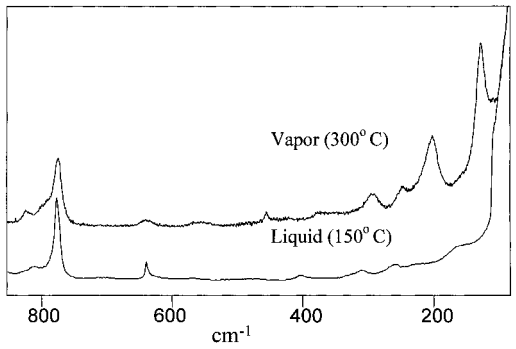

Figure 6. Vapor-phase Raman spectrum of DMS at 300 °C compared to its liquid (melt) spectrum at 150 °C.

as was shown in our studies of *trans*-stilbene and 4-methoxy-*trans*-stilbene.[2,3,7] Whereas the higher frequency bands for the solid, liquid, and vapor all have similar frequencies (confirming that the melt and vapor have not decomposed), the low-frequency bands for the vapor correspond to motions which are perturbed due to intermolecular interactions in the condensed phases. Table 4 presents the assignment of the low-frequency DMS modes based on the Raman spectra of the vapor and the fluorescence spectra (Figures 1 and 2). The corresponding frequencies for *trans*-stilbene and its methoxy derivative are also shown. As can be seen, there is considerable consistency in the vibrational frequencies for the three molecules.

Phenyl Torsions. The dispersed fluorescence spectra (SVLF) of *trans*-stilbene from the 0_0^0 origin showed bands at 19, 45, 76, and 108 cm^{-1} resulting from transitions to every other level of the ν_{37} phenyl torsion.[2] The SVLF from a hot band confirmed that there were also levels at 9, 31, 58, and 89 cm^{-1}. The ν_{48} phenyl torsion (in-phase) was observed at 118 cm^{-1}. In similar fashion the 0_0^0 band for methoxy-trans-stilbene[3] gave SVLF bands at 18, 42, and 73 cm^{-1} while the hot band showed other levels to be at 8, 30, 56, and 85 cm^{-1}. The ν_{48} torsion for the

TABLE 4: Low-Frequency Vibrational Assignments (cm^{-1}) for Dimethyl-*trans*-stilbene

			trans-stilbene		4-methoxy-*trans*-stilbene		dimethyl-*trans*-stilbene	
	approximate description		S_0	S_1	S_0	S_1	S_0	S_1
A_g	ν_{24}	Ce−Ph bend	273	280	234	279	201	228
	ν_{25}	phenyl wag	152	(150)[a]	144	(140)	125	122
A_U	ν_{35}	C═C torsion	101	99	86	85.5	87.5	89
	ν_{36}	phenyl flap	58	47.5	59	46	(58)	45
	ν_{37}	phenyl torsion	8	35	8	28	9	33
B_g	ν_{47}	phenyl flap	211	(200)	179	(170)	(212)	(200)
	ν_{48}	phenyl torsion	118	(110)	123	109	103	101
B_U	ν_{72}	phenyl wag	76	(70)	68	(63)	67	(60)
		methyl torsion					5.4	1.7

[a] Values in paretheses are estimated.

TABLE 5: Observed and Calculated Frequencies (cm^{-1}) for the Phenyl Torsions of 4,4′-Dimethyl-*trans*-stilbene

energy level[a]	S_0		S_1	
	obsd	calcd[b]	obsd	calcd[c]
(0,0)	0	0	0	0
(2,0)	(9)[d]	9	(33)	33
(4,0)	21	20	66	66
(6,0)	(33)	32	(99)	99
(8,0)	46	46	132	132
(10,0)	(59)	60		
(12,0)	73	75		
(0,2)	103	103	101	101

[a] The quantum numbers correspond to (ν_{37},ν_{48}). [b] $V_2 = 1550$; $V_{12} = 278$; $V'_{12} = 468$; $F_{11}^{(0)} = 0.8398059$; $F_{11}^{(2)} = 0.0230424$; $F_{11}^{(4)} = 0.0004138$; $F_{11}^{(c)} = 0.0024899$; $F_{11}^{(s)} = 0.0008383$; $F_{12}^{(0)} = 0.6686383$; $F_{12}^{(2)} = 0.0230424$; $F_{12}^{(4)} = 0.0004138$; $F_{12}^{(c)} = 0.002489$; $F_{12}^{(s)} = 0.0008383$ (all in cm^{-1}). [c] $V_2 = 1570$ cm^{-1}; $V_{12} = -110$ cm^{-1}; $V'_{12} = -110$ cm^{-1}; $F_{11}^{(0)} = 0.790683$; $F_{11}^{(2)} = 0.0219355$; $F_{11}^{(4)} = 0.0004054$; $F_{11}^{(c)} = 0.002405$; $F_{11}^{(s)} = 0.0007884$; $F_{12}^{(0)} = 0.6195156$; $F_{12}^{(2)} = 0.0219355$; $F_{12}^{(4)} = 0.0004054$; $F_{12}^{(c)} = 0.002405$; $F_{12}^{(s)} = 0.0007884$ (all in cm^{-1}). [d] Values in parentheses are determined indirectly or estimated.

S_0 state was found to be at 123 cm^{-1}. In the present work, due to the weakness of the SVLF spectra, only the ν_{37} levels at 21, 46, and 73 cm^{-1} were observed. The in-phase phenyl torsion was observed at 103 cm^{-1}. These data are nonetheless sufficient to allow a computation of the two-dimensional potential energy surface for the phenyl torsions of DMS. As before,[2,3] a computer program was written to calculate the kinetic energy expression for the two-dimensional problem. The potential energy expression

$$V(\phi_1,\phi_2) = \frac{1}{2}V_2(2 + \cos 2\phi_1 + \cos 2\phi_2) + V_{12}\cos 2\phi_1 \cos 2\phi_2 + V'_{12}\sin 2\phi_1 \sin 2\phi_2 \quad (2)$$

was then used to fit the experimental frequencies. The potential and kinetic energy parameters along with the calculated and observed frequencies are shown in Table 5, and the potential energy surface (PES) for the S_0 state is shown in Figure 7. This PES has a barrier to simultaneous phenyl torsion of 3100 cm^{-1}, while the barrier to internal rotation of a single phenyl group is 996 cm^{-1}. Both of these values were obtained by extrapolation so their accuracy is not very high (perhaps ±300 cm^{-1}). However, they do indicate that the substitution of the methyl groups on the benzene rings has very little effect on these barriers.

For the S_1 state the fluorescence excitation band at 66 cm^{-1} corresponds to the first observed ν_{37} level and shows the lowest level to be at 33 cm^{-1}. Other transitions listed in Table 1 show the first several levels to be nearly equally spaced, 33 cm^{-1} apart. The ν_{48} band is at 102 cm^{-1}. These data have also been fitted with the function of eq 2. Table 5 also lists the parameters and frequencies for the S_1 state and Figure 8 shows the PES. The barrier to planarity is 3140 cm^{-1} for the simultaneous torsion and 1790 cm^{-1} for a single internal rotation. These values are also very similar to those of the unsubstituted stilbene. Table 6 compares the barriers for the S_0 and S_1 states for the three stilbene molecules which have been studied.

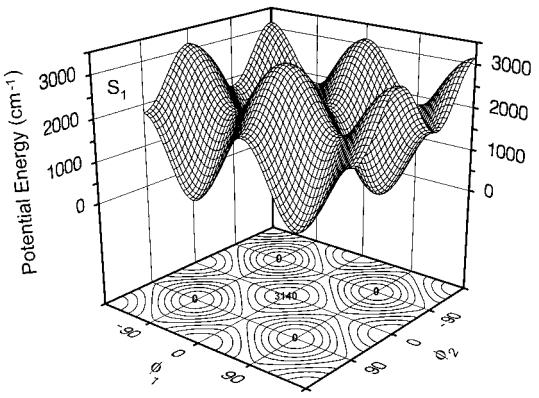

Figure 7. Potential energy surface for the phenyl torsions of DMS in its S_0 ground state.

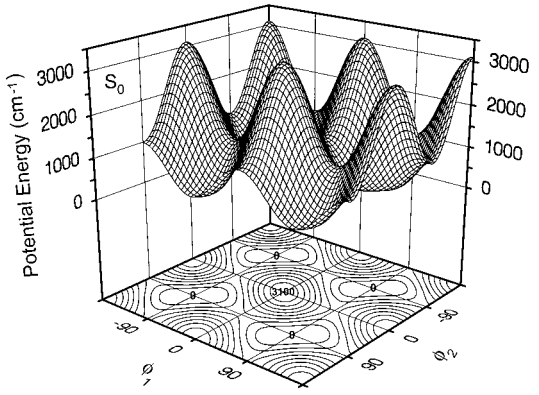

Figure 8. Potential energy surface for the phenyl torsions of DMS in its $S_1(\pi,\pi^*)$ excited state.

Ethylenic Torsion. Due to the complexity of the spectra arising from the many low-frequency vibrations, only one transition for the torsion about the C═C band can be assigned with some confidence. For S_0 the 0−2 separation is assigned to 173 cm^{-1}; for the S_1 excited state the 35_2^0 band is observed at 178 cm^{-1}. For *trans*-stilbene the corresponding values are 202 and 198 cm^{-1}, respectively; for 4-methoxy-*trans*-stilbene they are 172 and 171 cm^{-1}. The kinetic energy program previously used[2,3] was modified for DMS, and the *F* values for

TABLE 6: Phenyl Torsion Barriers (cm^{-1}) for *trans*-Stilbene

	S_0		S_1	
molecule	simultaneous internal rotation	single internal rotation	simultaneous internal rotation	single internal rotation
trans-stilbene	3100	875	3000	1670
4-methoxy-*trans*-stilbene	2860	1040	1040	1395
4,4′-dimethyl-*trans*-stilbene	3100	996	996	1790

the S_0 and S_1 states were calculated to be 0.126 for both states. The simple potential function

$$V(\mathrm{cm}^{-1}) = 7200(1 - \cos 2\phi) \qquad (3)$$

reproduces the observed transition for the S_0 state and corresponds to a barrier of 14 400 cm^{-1} (41 kcal/mol). However, as discussed previously,[2,3] the extrapolation of the PES to obtain the barrier height tends to produce too low a barrier by about 9%. Hence, the S_0 barrier is estimated to be 41 ± 5 kcal/mol. For *trans*-stilbene and its methoxy derivative the barriers were found to be 48.3 and 52.6 kcal/mol, respectively.

For the S_1 state there are again limited data for calculating the *trans*-twist barrier. However, analogy with the previously studied molecules allows a range for the barrier to be estimated. The 175 cm^{-1} band corresponds to a 87.5 cm^{-1} first quantum state in the trans well which can correspond to a barrier of about 2400 ± 1000 cm^{-1}. Thus, there is an apparent increase over the barrier for *trans*-stilbene, but the lack of assigned higher level transitions makes it impossible to determine this very accurately.

Conclusions

The fluorescence excitation spectrum of DMS is strong but very congested due to the large number of low-frequency vibrations in the molecule. The dispersed fluorescence spectra from individual excitation lines are weak. Analysis of the data shows that the phenyl torsions, the torsion about the C═C bond, and the other low-frequency vibrations of DMS are all similar to those of *trans*-stilbene and its methoxy derivative. The barriers to phenyl torsion, which are shown in Table 6 and which are all obtained by extrapolation, are very similar and agree with one another within experimental uncertainty indicating that substitution has a limited effect on these internal rotations. Similarly, the substitution only appears to have a minor effect on the torsion about the ethylinic bond although there appears to be a small decrease in the barrier for the S_0 state, and a possible small increase for the S_1 state.

The quantum states determined for the methyl internal rotations showed the two rotors to be uncoupled, and the energy levels were found to be very similar to those of *m*-xylene. In the S_0 state, the internal rotation is essentially free ($V_6 = 15 \pm 15$ cm^{-1}) while the S_1 state has a small 3-fold barrier ($V_3 = 85 \pm 10$ cm^{-1}; $V_6 = -30 \pm 20$ cm^{-1}). As was the case for the xylenes, the electronic excitation not only increases the barrier but also results in it being primarily 3-fold in character.

Acknowledgment. J. L. thanks the National Science Foundation, Robert A. Welch Foundation, and the Texas Advanced Research Program for financial support.

References and Notes

(1) Waldeck, D. H. *Chem. Rev.* **1991**, *91*, 415 and references therein.
(2) Chiang, W.-Y.; Laane, J. *J. Chem. Phys.* **1994**, *10*, 8755 and references therein.
(3) Chiang, W.-Y.; Laane, J. *J. Phys. Chem.* **1995**, *99*, 11823.
(4) Drefahl, G.; Ploetner, G. *Chem. Ber.* **1958**, *91*, 1274.
(5) Cheatham, C. M.; Huang, M.-H.; Laane, J. *J. Mol. Struct.* **1996**, *377*, 93.
(6) Cheatham, C. M.; Huang, M.-H.; Meinander, N.; Kelly, M. B.; Haller, K.; Chiang, W.-Y.; Laane, J. *J. Mol. Struct.* **1996**, *377*, 81.
(7) Haller, K.; Chiang, W.-Y.; del Rosario, A.; Laane J. *J. Mol. Struct.* **1996**, *379*, 19.
(8) Breen, P. J.; Warren, J. A.; Bernstein, E. R.; Seeman, J. I. *J. Chem. Phys.* **1987**, *87*, 1917.
(9) Suzuki, T.; Ikegami, T.; Fujii, M.; Iwata, S. *J. Mol. Struct. (THEOCHEM)* **1998**, *461−462*, 79.
(10) Held, A.; Seizle, H. L.; Schlag, E. W. *J. Phys. Chem.* **1998**, *102*, 9625.
(11) Lewis, J. P.; Malloy, T. B.; Chao, T.; Laane, J. *J. Mol. Struct.* **1972**, *12*, 427.
(12) Sakamoto, A.; Tasumi, M. Unpublished results.